

Journal Pre-proof

Assessment of normal pulmonary development using functional MRI techniques

Carla L. Avena-Zampieri , Jana Hutter , Maria Deprez ,
Kelly Payette , Megan Hall , Alena Uus , Surabhi Nanda ,
Anna Milan , Paul T Seed , Mary Rutherford , Anne Greenough ,
Lisa Story

PII: S2589-9333(23)00077-0
DOI: <https://doi.org/10.1016/j.ajogmf.2023.100935>
Reference: AJOGMF 100935



To appear in: *American Journal of Obstetrics & Gynecology MFM*

Received date: 6 January 2023
Revised date: 10 March 2023
Accepted date: 13 March 2023

Please cite this article as: Carla L. Avena-Zampieri , Jana Hutter , Maria Deprez , Kelly Payette , Megan Hall , Alena Uus , Surabhi Nanda , Anna Milan , Paul T Seed , Mary Rutherford , Anne Greenough , Lisa Story , Assessment of normal pulmonary development using functional MRI techniques, *American Journal of Obstetrics & Gynecology MFM* (2023), doi: <https://doi.org/10.1016/j.ajogmf.2023.100935>

This is a PDF file of an article that has undergone enhancements after acceptance, such as the addition of a cover page and metadata, and formatting for readability, but it is not yet the definitive version of record. This version will undergo additional copyediting, typesetting and review before it is published in its final form, but we are providing this version to give early visibility of the article. Please note that, during the production process, errors may be discovered which could affect the content, and all legal disclaimers that apply to the journal pertain.

© 2023 The Author(s). Published by Elsevier Inc.

This is an open access article under the CC BY license (<http://creativecommons.org/licenses/by/4.0/>)

Assessment of normal pulmonary development using functional MRI techniques

Carla L. Avena-Zampieri^{1,2}, Jana Hutter², Maria Deprez^{2,7}, Kelly Payette^{2,7}, Megan Hall^{1,2,3}, Alena Uus^{2,7}, Surabhi Nanda³, Anna Milan⁴, Paul T Seed¹, Mary Rutherford², Anne Greenough^{1,5,6}, Lisa Story^{1,2,3}

¹ Department of Women and Children's Health King's College London

² Centre for the Developing Brain, School of Biomedical Engineering & Imaging Sciences, King's College London

³ Fetal Medicine Unit, Guy's and St Thomas' NHS Foundation Trust

⁴ Neonatal Unit, Guy's and St Thomas' NHS Foundation Trust

⁵ Neonatal Unit, King's College Hospital

⁶ NIHR Biomedical Research Centre based at Guy's & St Thomas NHS Foundation Trusts and King's College London

⁷ Department of Biomedical Engineering, School of Biomedical Engineering & Imaging Sciences, King's College London

Conflict of Interest Statement

The authors have no conflicts of interest to declare.

Funding Sources

- Dr Lisa Story, NIHR Advanced Fellow, is funded by Health Education England (HEE) / National Institute for Health Research (NIHR) for this research project. The views expressed in this publication are those of the authors and not necessarily those of the NIHR, NHS or the UK Department of Health and Social Care.
- Dr Jana Hutter is supported by core funding from the Wellcome/EPSRC Centre for Medical Engineering [WT203148/Z/16/Z], by the NIH Human Placenta Project grant 1U01HD087202-01 (Placenta Imaging Project (PIP)), by the Wellcome Trust, Sir Henry Wellcome Fellowship to JH, [201374/Z/16/Z], by the UKRI, FLF to JH [MR/T018119/1] and by the National Institute for Health Research (NIHR) Biomedical Research Centre based at Guy's and St Thomas' NHS Foundation Trust and King's College London.

Corresponding author:

Carla Avena-Zampieri

Department of Women's and Children's Health

St Thomas' Hospital

London

SE1 7EH

carla.avena_zampieri@kcl.ac.uk

Assessment of normal pulmonary development using functional MRI techniques

The current article is an expert opinion which reviews the available methods to non-invasively characterise the fetal developing lungs, exposing the most effective and innovative methodologies applicable.

Condensation: Mean pulmonary T2* values in healthy fetuses were found to increase with advancing gestational age between 20-38 weeks.

AJOG at a glance:

A) Why was this study conducted? This study was conducted to assess normal fetal pulmonary development across gestation using an advanced functional MRI imaging technique, T2*, potentially reflective of oxygenation and alterations in pulmonary tissue composition across gestational age.

B) What are the key findings? We demonstrated that between 20 –38 weeks' gestation, mean T2* values increased.

C) What does this study add to what is already known?

This study provides original motion-corrected morphological and functional assessment of the antenatal fetal lung during normal development. This will form the basis of reference ranges to assess fetuses who may have compromised pulmonary growth and function

The authors have no conflicts of interest to declare.

Funding Sources

- Author 11, NIHR Advanced Fellow, is funded by Health Education England (HEE) / National Institute for Health Research (NIHR) for this research project. The views expressed in this publication are those of the authors and not necessarily those of the NIHR, NHS or the UK Department of Health and Social Care.
- Author 2 is supported by core funding from the Wellcome/EPSRC Centre for Medical Engineering [WT203148/Z/16/Z], by the NIH Human Placenta Project grant 1U01HD087202-01 (Placenta Imaging Project (PIP)), by the Wellcome Trust, Sir Henry Wellcome Fellowship to JH, [201374/Z/16/Z], by the UKRI, FLF to JH [MR/T018119/1] and by the National Institute for Health Research (NIHR) Biomedical Research Centre based at Guy's and St Thomas' NHS Foundation Trust and King's College London.

Word Count: Abstract - 321; Main Text – 2655

Abstract

Background

The mainstay of assessment of the fetal lungs in clinical practice is via evaluation of pulmonary size, primarily using 2D ultrasound and more recently with anatomical MRI. The emergence of advanced MR techniques such as T2* relaxometry in combination with the latest motion correction post-processing tools now facilitates assessment of the metabolic activity/perfusion of fetal pulmonary tissue in vivo.

Objective

To characterise normal pulmonary development using T2* relaxometry, accounting for fetal motion, across gestation.

Methods

Datasets were analysed from women with uncomplicated pregnancies that delivered at term. All subjects had undergone T2-weighted imaging and T2* relaxometry on a Phillips 3T MRI system antenatally. T2* relaxometry of the fetal thorax was performed using a gradient echo single-shot echo planar imaging sequence. Following correction for fetal motion using slice-to-volume reconstruction, T2* maps were generated using in-house pipelines. Lungs were manually segmented and mean T2* values calculated for the right and left lungs individually, and both lungs combined. Lung volumes were generated from the segmented images and right, left and both lungs combined were also assessed.

Results

Eighty-seven datasets were suitable for analysis. The mean gestation at scan was 29.9 ± 4.3 weeks (range: 20.6-38.3) and mean gestation at delivery was 40 ± 1.2 weeks (range: 37.1-42.4). Mean T2* values of the lungs increased over gestation for right and left individually and for both lungs assessed together ($p=0.003$; $p=0.04$; $p=0.003$). Right, left, and total lung volumes were also strongly correlated with increasing gestational age ($p < 0.001$ in all cases).

Conclusions:

This is the largest study to date assessing the developing lungs using T2* imaging across a wide gestational age range. Mean T2* values increased with gestational age which may reflect increasing perfusion and metabolic requirements and alterations in tissue composition as gestation advances. In the future, evaluation of findings in fetuses with conditions known to be associated with pulmonary morbidity may lead to enhanced prognostication antenatally consequently improving counselling and perinatal care planning.

Keywords: Lung development, fetal MRI, prenatal prediction, T2*

Background

Normal lung development encompasses five principal stages and disruption at any of these time points can result in mortality or significant long-term pulmonary morbidity. Lung growth commences during the embryonic stage (three-seven weeks of development). This initial stage is characterised by vascularisation and formation of smooth muscle within the airways, tracheal cartilage, and pleura. The second, pseudo-glandular stage encompasses the seven to 16 week period. During this time, formation of the conducting airways to the level of the terminal bronchioles is complete and 75% of bronchial branching has occurred¹. Vascularisation increases during the canicular stage (weeks 16-28) and by the end of this period gaseous exchange becomes feasible. Also, during this time, the first zones with an alveolar-capillary barrier start to develop. The period between 28 and 36 weeks, the sacular stage, is a transitional period. Terminal sacs form and biochemical lung maturation occurs. Type II pneumocytes now secrete surfactant which reduces pulmonary surface tension. Mature alveoli do not form until after birth, the last stage of lung growth (alveolar) comprises development of the final alveolar sacs and is accompanied by a gradual increase in lung volume.

Current assessment of the fetal lungs in clinical practice is limited to the evaluation of size, most commonly using two-dimensional ultrasound measures but also via three-dimensional volumes derived either from ultrasound or MRI²⁻⁴. Although these assessment tools are useful and have been validated for prognostication of congenital diaphragmatic hernia, their clinical utility is limited given their paucity in demonstrating accurate prognostic value in other pulmonary disorders such as pulmonary hypoplasia associated with second trimester preterm prelabour rupture of the membranes⁵.

Fetal MRI is a rapidly evolving field and recent advances include bespoke techniques for both acquisition and analysis. These include the application of functional acquisition techniques, such as T2* relaxometry, as well as the emergence of sophisticated motion correction pipelines including deformable slice to volume reconstruction (DSVR)^{6,7}. T2* relaxation refers to the decay of transverse magnetization seen with gradient-echo (GRE) sequences⁸. T2* relaxometry utilises the fact that oxygenated and deoxygenated haemoglobin have different paramagnetic properties and therefore provides an indirect assessment of tissue perfusion. Mean T2* quantitative values can be acquired for a specific region of tissue and a map can be generated illustrating regional variations of oxygenation. This technique has already been utilised during pregnancy to investigate placental pathology associated with conditions such as pre-eclampsia and chronic hypertension^{9,10}. Normal T2* values have also been evaluated in healthy pregnancies in the second and third trimesters in fetal organs such as the brain¹¹ and liver¹². However, only one small study to date, comprising of only nine participants, has evaluated the fetal lungs using T2* relaxometry¹³.

This project aims to comprehensively assess fetal mean pulmonary T2* values across gestation in a large cohort of uncomplicated pregnancies to assess normal pulmonary development.

Methods

A retrospective study was performed by selecting a control cohort from three studies (REC: 16/LO/1573, IRAS 201609), (19/LO/0736, IRAS 253500) and (REC: 21/SS/0082, IRAS 293516), undertaken at St Thomas' Hospital over a 4-year period from 2018 to 2022.

Inclusion criteria included: women with singleton, uncomplicated pregnancies with no pre-existing medical conditions who subsequently delivered their babies after 37 weeks' gestation with no neonatal complications. Exclusion criteria for MRI included: women who had claustrophobia or a recently sited metallic implant. Cases with a birthweight centile <3rd or >97th centile (calculated using the INTERGROWTH centiles)¹⁴, as these may have had underlying pathology. Cases were additionally excluded where MRI data was found to be corrupted or subject to excessive motion or where outcome data was incomplete.

All women underwent imaging on a clinical 3T Philips MRI scanner using a 32-channel cardiac coil in a supine position¹⁵. Heart rate and intermittent blood pressure readings were performed during the scan and frequent verbal interaction was maintained. Demographic, delivery, and postnatal data, including maternal age, ethnicity, body mass index, gestational age at delivery, birthweight and neonatal outcome of all pregnancies were collected from clinical maternity and infant records with participant consent.

Anatomical imaging of the fetal thorax was performed using a T2-weighted single-shot turbo spin echo sequence acquired in three orthogonal planes focused on the fetal body and an additional whole uterus coronal plane¹⁶. After acquisition of a B0 map, manual image-based shimming was performed using an in-house tool¹⁷. A multi-echo gradient echo single-shot echo planar sequence was then performed with the following parameters: 3mm³ resolution, five echo times [13.8 ms / 70.4 ms / 127.0 ms / 183.6 ms / 240.2 ms], repetition time (TR) = 3 seconds, parallel imaging SENSE factor = 3, flip angle = 90°. The field of view was set to 360 mm × (320–400) mm × (60–120) mm using a coronal imaging plane aligned to the scanner co-ordinates, in order to encompass the whole thorax and minimise artefacts from parallel imaging reconstruction techniques. The imaging protocol, including additional techniques such as diffusion MRI, dynamic imaging and perfusion imaging, was completed within one hour in all cases and women were offered a break midway through.

As previously described, an in-house Python script was used to generate T2* maps using mono-exponential decay fitting¹⁶. Another in-house pipeline, DSVR¹⁸, has been previously used to generate reconstructed abdominal and thoracic images to account for unpredictable fetal motion. This technique was previously validated in fetal MRI for volumetric analysis from multiple stacks of slices⁶, and was applied to the datasets. It facilitates correction of both in- and out-of-plane local deformations of fetal organs caused by bending and stretching motions and hence renders segmentations more accurate. (Figure 1.a)

Raw stacks used for reconstruction with satisfactory quality (where motion artefact was evident or the imaging of the thoracic region was incomplete were discarded) and where data for both lungs was available, were inspected and selected. The motion patterns obtained from the DSVR were applied to the spatially matched T2* maps. The resulting reconstructed images (an example of which is seen in Figure 1.b) were also inspected for adequate quality. The adequate 3D reconstruction quality implies minimal impact of fetal motion (if some remaining), clear definition and visibility of both lungs without motion sufficient for detailed delineation of lung tissue. Lung tissue segmentation was performed using the computer

software 3D Slicer¹⁹ on the 3D reconstructed images. Manual segmentation of the lungs was performed by an experienced observer carefully avoiding any non-pulmonary tissue (Figure 2) (intensity range was adjusted to adapt the visualisation and make segmentation easier by increasing contrast between pulmonary tissue and other structures, for example vascular structures and amniotic fluid).

Mean T2* values, lung volumes and lacunarity scores (reflective of changes in granularity and heterogeneity of tissue²⁰) were obtained and corresponding histograms were generated using a purpose-built Python script^{16,21}. Additionally, T2* maps were assessed visually in order to provide a perceptible representation of heterogeneity of tissue oxygenation within the lungs. Cases were selected to give a visual representation of the changes over gestational age by selecting one per week to display the main lung stages of pulmonary development.

Applying the same segmentation methodology, we additionally obtained mean pulmonary T2* values from the raw images from 10 cases as well as the reconstructed images to assess the influence that motion correction had on the absolute T2* values.

Intra- and inter-observer variability assessment of pulmonary T2* values, volumes and their 95% confident intervals, were calculated using an absolute-agreement 2 way mixed-effects model in SPSS statistical package version 28.0.1 (SPSS IBM). Further statistical analysis was performed using Scipy in Python 3. Linear regression analysis was performed for lung volumes and T2* values in both lungs, right and left lung separately, to assess the relationship between gestational age and pulmonary parameters. In addition, parameters for the right and left lung were compared. Ten of the women had a maximum of two scans in the course of their pregnancies. We therefore accounted for serial measures by adjusting the standard errors and for clustering. The results remained significant, all demonstrating that both mean and standard deviation increase with gestation. Additionally we carried out an analysis which led to a method for converting lung T2* to a Z-score (observed fetal T2* – mean)/SD for a given result), which can be converted to centiles using normal distribution. Centiles could be derived from converting lung T2* values to z-scores and yielded the following for the mean $1.488884 * (\text{gestational age of scan in weeks}) + 21.997645$ and standard deviation $1.488884 * (\text{gestational age of scan in weeks}) - 18.451005$.

Results

Eighty-seven datasets were suitable for analysis. Eighteen had been excluded: eight due to incomplete clinical outcome data, seven due to significant motion corruption, for which the motion correction pipelines could not compensate, and three due to incomplete imaging of the fetal thorax (as the fetal thorax was not the primary region of interest of two of the studies from which data were included) (Figure 3). Maternal demographics and neonatal outcomes of the cohort can be seen in Table 1. All of the neonates had an uncomplicated course post-delivery and did not require any form of respiratory support.

Results for each lung, and both combined, were obtained from 20.6 to 38.3 weeks' gestation. T2* values positively correlated with gestational age in each lung separately and combined, with no difference observed between the right and left lungs ($p=0.0001$; slope= 1.61; intercept= 19.61; R-squared= 0.13), right lung ($p= 0.005$; slope=1.20; intercept= 28.98; R-squared= 0.08) and left lung ($p=0.0006$; slope= 1.51; intercept= 22.80; R-squared= 0.11)

(Figure 4/5). Likewise, lacunarity scores increased with gestation (Figure 6) (both lungs ($p < 0.001$), right lung ($p < 0.001$) and left lung ($p < 0.001$)). Visual inspection of maps reveals increasing heterogeneity with gestation (Figure 7). Finally, as expected, lung volumes increased with gestation (total, right and left lungs ($p < 0.001$, $p < 0.001$ and $p < 0.001$)) (Figure 8).”

Intra- and inter-observer variability was good for both volume and mean T2* values. Intra observer variability had an ICC of 0.989 for volume and 0.998 for mean T2* and inter observability had an ICC of 0.951 for volume and 0.997 for mean T2*

Discussion

Significant findings and results

In 87 healthy pregnancies we have demonstrated that antenatal mean pulmonary T2* values increase with increasing gestational age between 20- and 38-weeks’ gestation in right and left lungs separately, and both lungs combined. Pulmonary volumes were also found to increase with gestation with lower volumes in the left lung compared to the right (Figure 8).

These findings are in contrast to the only previously published study assessing pulmonary T2* values in the antenatal period¹³. Sethi et al reported no variation in T2* values across gestation in total lung tissue. However, their sample size comprised of only nine fetuses, in comparison with the 87 included in our study. The gestational period assessed was also narrower (28-38 weeks, in comparison with 20.6-38.3 weeks) both of which may explain the differing findings. The mean T2* values appeared to be higher in our study for comparable gestational ages than in the work by Sethi et al¹³. This may be explained in part, by the fact that our study was conducted on a 3T MRI system in contrast to a 1.5T used by their group. Higher field strength is associated with higher T2* values²². Increased dephasing occurs at higher field strengths due to susceptibility effects and increased inhomogeneity in the magnetic fields of the magnet. Differences in acquisition protocols, i.e. TRs (repetition times) and TEs (time to echo), field of view and differing tools for image-based shimming, may also influence to a lesser extent the differences observed in T2* values between the two studies.

Unlike previous studies which have utilised T2* to assess fetal lungs, and structures, such as the brain ¹¹, liver ¹² spleen ¹³ and lung ¹³ our study also accounted for fetal motion using the DSVR post-processing technique ⁶. Fetal MRI and quantitative T2* analysis are particularly susceptible to motion. Using raw datasets may mean that non pulmonary tissue was included and smaller structures such as vessels may inadvertently have been part of the segmentations thus rendering results inaccurate. Although the application of DSVR pipelines results in altered, higher, tissue resolution which may affect the T2* values obtained, we found no statistical difference between mean T2* datasets obtained from the raw data in comparison with those obtained following the DSVR pipeline.

Research and clinical implications

T2* values are obtained from the combined effects of spin-spin relaxation (T2) and magnetic field inhomogeneity ⁸, hence T2 and T2* values are inherently related. T2* values within tissues are attributable to the effect of magnetic field inhomogeneities, for example arising from the paramagnetic properties of deoxygenated haemoglobin in comparison with oxygenated haemoglobin. In addition, T2* values are also affected by elements of tissue composition (the intrinsic T2 value) such as cell density, water or fluid content, and surface area. An increase in T2* values in the fetal lungs with advancing gestational age may be partly related to altering tissue and fluid composition as gestation progresses. These findings are consistent with the increase of T2 values, attributed to developmental changes, in the fetal lungs from 19 to 40 weeks studied in 105 healthy pregnancies by Cannie et al ²³.

As gestation increases, an increasing proportion of cardiac output is directed to the fetal lungs²⁴ ranging from 13% between 16 and 28 weeks to 30% between 28 and 36 weeks²⁵. Fetal haemoglobin concentration is constant from approximately 10 weeks' gestation until 24 weeks. Although concentrations then decline towards term adult haemoglobin concentrations increase from approximately 31 weeks²⁶. This might affect T2* values, similarly to the changes in geometry related to the development of the pulmonary vascular tree such as increased capillary density within each MR voxel. Lacunarity scores reflect changes in granularity and tissue heterogeneity. We demonstrated a significant correlation with gestational age for both lungs, which again, may in part be related to the maturation of the pulmonary vascular tree reflected in the T2* values recorded.

A diverse range of processes are known to alter the MR properties of pulmonary parenchyma across gestation. Developmental processes include angiogenesis, development of the alveoli and bronchioles and alterations of pulmonary tissue content. These require cellular proliferation and differentiation associated with an increased metabolic demand and tissue perfusion. In addition, the fluid composition of the lungs also alters with gestation, lung fluid secretion decreases, and sodium transport dependent resorption increases which facilitates gaseous exchange after birth²⁷. An increase in surfactant production and therefore concentration of phospholipids, lipids and proteins content is also known to occur with increasing gestation. Maturation of the pulmonary structural components includes not only the microvasculature but also the extracellular matrix, composed of a complex mixture of fibrous proteins. Since the extracellular matrix governs many fundamental cellular processes (including alveolar septation), especially during the saccular phase, those processes might be reflected in the T2* values recorded. All these physiological changes may therefore also affect T2* values across gestation.

The pulmonary volumes obtained in our study were lower than previously reported²⁸⁻³⁰, however, this is most likely attributable to the conservative segmentation deployed in order to ensure only pulmonary tissue was included. We therefore propose that where absolute lung volumes are required these are optimally obtained from T2 datasets as opposed to the T2* datasets.

Strengths and Limitations

This is the largest study characterising pulmonary development across gestation using mean T2* encompassing 87 healthy pregnancies between 20.6- and 38.3-weeks gestation. Utilising DSVR post-processing pipelines facilitated correction for motion and distortion deterioration. We have demonstrated excellent reliability scores, making this technique reproducible and valuable for future applications. However, assessment of pulmonary T2* values provides an indirect assessment of tissue perfusion only and the application of DSVR may also alter the mean values of T2* due to interpolation effects applied during the super resolution as it attempts to reconstruct the original scene image with high resolution. Although a large gestational age range has been encompassed within this study, no datasets were included prior to 20 weeks or after 39 weeks gestation. Further work focusing on these periods should be conducted in order to provide a complete assessment of in-utero pulmonary development. It should also be noted that the majority of women participating in this study are white. It is therefore imperative that further work should assess a diverse population to ensure that findings are applicable to all ethnic groups.

Conclusion and clinical implications

Our results have given functional insight into pulmonary development potentially reflecting increased perfusion and metabolic activity of tissue as gestation advances. Investigation of fetuses at high risk of pulmonary morbidity using these techniques will be required to assess if alterations in pulmonary T2* values are associated with pathology. If this is found to be the case the role of T2* as a prognostic marker can then be assessed.

References

1. SCHITTNY JC. Development of the lung. *Cell Tissue Res* 2017;367:427-44.
2. OKA Y, RAHMAN M, SASAKURA C, et al. Prenatal diagnosis of fetal respiratory function: evaluation of fetal lung maturity using lung-to-liver signal intensity ratio at magnetic resonance imaging. *Prenatal diagnosis* 2014;34:1289-94.
3. LIAN X, XU Z, ZHENG L, et al. Reference range of fetal thorax using two-dimensional and three-dimensional ultrasound VOCAL technique and application in fetal thoracic malformations. *BMC Med Imaging* 2021;21:34.
4. PERALTA CFA, CAVORETTO P, CSAPO B, VANDECRUYS H, NICOLAIDES KH. Assessment of lung area in normal fetuses at 12–32 weeks. *Ultrasound in Obstetrics & Gynecology* 2005;26:718-24.
5. VAN TEEFFELN AS, VAN DER HEIJDEN J, OEI SG, et al. Accuracy of imaging parameters in the prediction of lethal pulmonary hypoplasia secondary to mid-trimester prelabor rupture of fetal membranes: a systematic review and meta-analysis. *Ultrasound Obstet Gynecol* 2012;39:495-9.
6. UUS A, STEINWEG JK, HO A, et al. *Deformable Slice-to-Volume Registration for Reconstruction of Quantitative T2* Placental and Fetal MRI*. Cham: Springer International Publishing, 2020.
7. DAVIDSON J, UUS A, EGLOFF A, et al. Motion corrected fetal body magnetic resonance imaging provides reliable 3D lung volumes in normal and abnormal fetuses. *Prenatal Diagnosis* 2022;42:628-35.
8. CHAVHAN GB, BABYN PS, THOMAS B, SHROFF MM, HAACKER EM. Principles, techniques, and applications of T2*-based MR imaging and its special applications. *Radiographics* 2009;29:1433-49.
9. HO AEP, HUTTER J, JACKSON LH, et al. T2* Placental Magnetic Resonance Imaging in Preterm Preeclampsia: An Observational Cohort Study. *Hypertension* 2020;75:1523-31.

10. HO A, HUTTER J, SLATOR P, et al. Placental magnetic resonance imaging in chronic hypertension: A case-control study. *Placenta* 2021;104:138-45.
11. BLAZEJEWSKA AI, SESHAMANI S, MCKOWN SK, et al. 3D in utero quantification of T2* relaxation times in human fetal brain tissues for age optimized structural and functional MRI. *Magn Reson Med* 2017;78:909-16.
12. GOITEIN O, ESHET Y, HOFFMANN C, et al. Fetal liver T2* values: defining a standardized scale. *J Magn Reson Imaging* 2013;38:1342-5.
13. SETHI S, GIZA S, GOLDBERG E, et al. Quantification of 1.5 T T1 and T2* Relaxation Times of Fetal Tissues in Uncomplicated Pregnancies. *Journal of magnetic resonance imaging : JMRI* 2021;54.
14. VILLAR J, ISMAIL LC, VICTORA CG, et al. International standards for newborn weight, length, and head circumference by gestational age and sex: the Newborn Cross-Sectional Study of the INTERGROWTH-21st Project. *The Lancet* 2014;384:857-68.
15. HUGHES EJ, PRICE AN, MCCABE L, et al. The effect of maternal position on venous return for pregnant women during MRI. *NMR Biomed* 2021;34:e4475.
16. HUTTER J, SLATOR PJ, JACKSON L, et al. Multi-modal functional MRI to explore placental function over gestation. *Magn Reson Med* 2019;81:1191-204.
17. GASPAR AS, NUNES RG, FERRAZZI G, et al. Optimizing maternal fat suppression with constrained image-based shimming in fetal MR. *Magn Reson Med* 2019;81:477-85.
18. UUS A, ZHANG T, JACKSON LH, et al. Deformable Slice-to-Volume Registration for Motion Correction of Fetal Body and Placenta MRI. *IEEE transactions on medical imaging* 2020;39:2750-59.
19. FEDOROV A, BEICHEL R, KALPATHY-CRAMER J, et al. 3D Slicer as an image computing platform for the Quantitative Imaging Network. *Magn Reson Imaging* 2012;30:1323-41.
20. PRAKASH KN, RAMAKRISHNAN AG, SURESH S, CHOW TW. An investigation into the feasibility of fetal lung maturity prediction using statistical textural features. *Ultrason Imaging* 2001;23:39-54.
21. HUTTER J, JACKSON L, HO A, et al. T2* relaxometry to characterize normal placental development over gestation in-vivo at 3T. *Wellcome Open Research* 2019;4.
22. KIDAMBI A, BIGLANDS JD, HIGGINS DM, et al. Susceptibility-weighted cardiovascular magnetic resonance in comparison to T2 and T2 star imaging for detection of intramyocardial hemorrhage following acute myocardial infarction at 3 Tesla. *J Cardiovasc Magn Reson* 2014;16:86.
23. CANNIE M, JANI J, DE KEYZER F, ROEBBEN I, BREYSEM L, DEPREST J. T2 quantifications of fetal lungs at MRI-normal ranges. *Prenatal Diagnosis* 2011;31:705-11.
24. LAKSHMINRUSIMHA S, SAUGSTAD OD. The fetal circulation, pathophysiology of hypoxemic respiratory failure and pulmonary hypertension in neonates, and the role of oxygen therapy. *Journal of Perinatology* 2016;36:S3-S11.
25. LUMB AB, SLINGER P. Hypoxic Pulmonary Vasoconstriction: Physiology and Anesthetic Implications. *Anesthesiology* 2015;122:932-46.
26. ILEANA C, SJAAK P. Flicking the switch: adult hemoglobin expression in erythroid cells derived from cord blood and human induced pluripotent stem cells. *Haematologica* 2014;99:1647-49.
27. WEDEGAERTNER U, TCHIRIKOV M, HABERMANN C, et al. Fetal Sheep with Tracheal Occlusion: Monitoring Lung Development with MR Imaging and B-Mode US. *Radiology* 2004;230:353-58.

28. STORY L, ZHANG T, STEINWEG JK, et al. Foetal lung volumes in pregnant women who deliver very preterm: a pilot study. *Pediatric Research* 2020;87:1066-71.
29. MEYERS ML, GARCIA JR, BLOUGH KL, ZHANG W, CASSADY CI, MEHOLLIN-RAY AR. Fetal Lung Volumes by MRI: Normal Weekly Values From 18 Through 38 Weeks' Gestation. *AJR Am J Roentgenol* 2018;211:432-38.
30. CANNIE MM, JANI JC, KERKHOVE FV, et al. Fetal Body Volume at MR Imaging to Quantify Total Fetal Lung Volume: Normal Ranges. *Radiology* 2008;247:197-203.

Figure Legends

Figure 1. *MRI images of the fetal thorax acquired on a 3 Tesla system. Row A illustrates the native slice-plane and row B illustrates the corresponding view after deformable slice to volume reconstruction. The first column indicates the sagittal plane, the second column the axial plane and the third column the coronal plane.*

Figure 2. *Illustrating a manual segmentation of fetal lung tissue on the 3D reconstructed image in the axial, sagittal and coronal planes. The pink illustrates right lung tissue and red illustrates left lung tissue (segmented conservatively to avoid the vasculature in black).*

Table 1. *Clinical characteristics study cohort*

Figure 3. *Flowchart of the data selection process*

Figure 4. *Mean pulmonary T2* values over gestational age at scan in right lung (red dots), left lung (blue crosses) and both lungs combined (black triangles)*

Figure 5. *Histograms to illustrate the distribution of pulmonary T2* voxel values from the right (right) and left (left) lungs, from all participants, (lighter curves represent earlier gestational ages at scan).*

Figure 6. *Scatterplot of lacunarity measure (derived from T2* mapping) for right (red dot), left (blue cross) and both lungs (black triangle).*

Figure 7. *T2* maps in axial, sagittal and coronal views of fetal lungs in normal pregnancies with a gestational age at scan range of 22.4-38.3. The scale of T2* values is displayed where red colours are low and yellow are high.*

Figure 8. *Pulmonary volumes over gestational age at scan in right (red dot), left (blue cross) and both lungs (black triangle).*

Supplementary figure legends

Supplementary figure 1. *Comparison of mean pulmonary T2* values obtained after 3D reconstruction (green) and raw stacks (blue) for each of the 10 cases.*

Supplementary figure 2. *Longitudinal data of 10 of the cases over gestation with a repeated scan in the course of their pregnancy. A) represents the first scans and B) the second scans.*

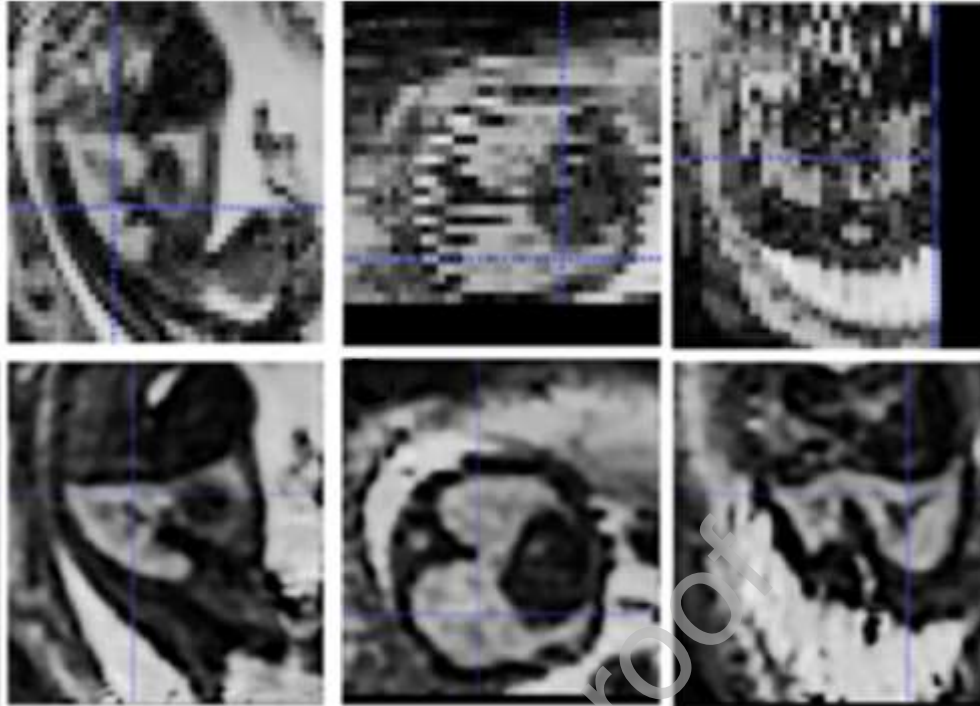


Figure 1: T2* MRI images of the fetal thorax acquired on a 3 Tesla system. Row A illustrates the native slice-plane and row B illustrates the corresponding view after deformable slice to volume reconstruction. The first column indicates the sagittal plane, the second column the axial plane and the third column the coronal plane.

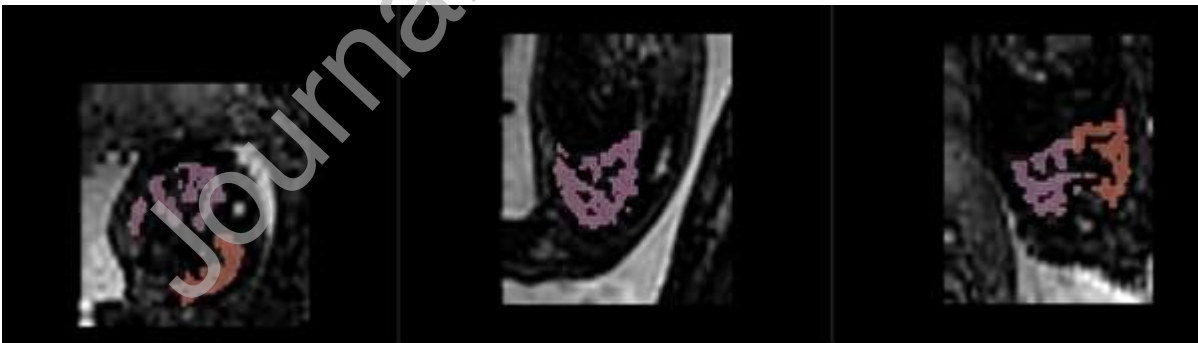


Figure 2: Illustrating a manual segmentation of fetal lung tissue on the 3D reconstructed image in axial, sagittal and coronal planes. The pink illustrates right lung tissue and red illustrates left lung tissue (segmented conservatively to avoid the vasculature in black).

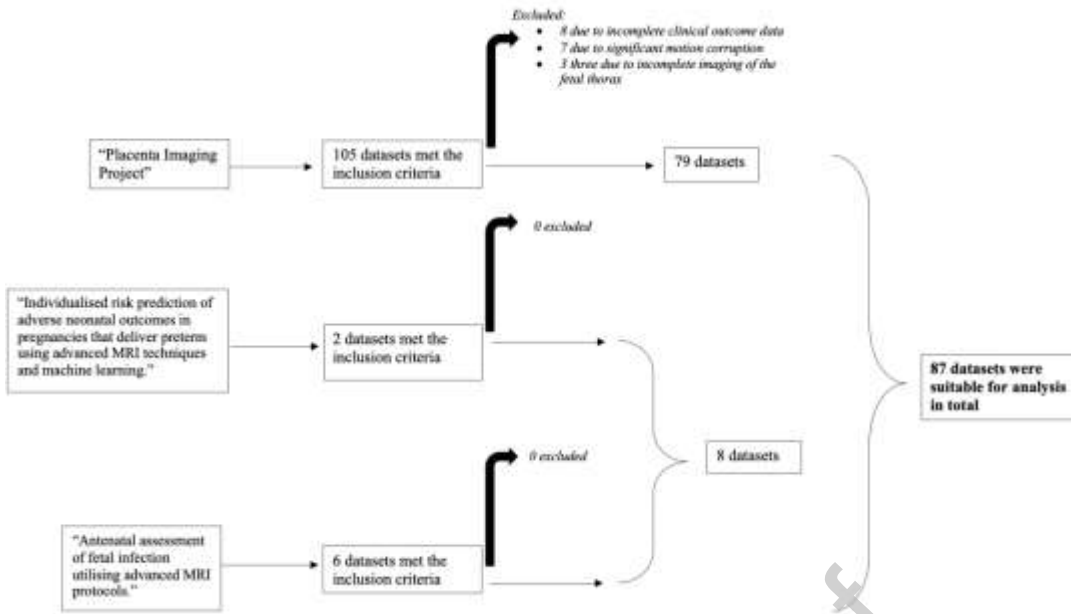


Figure 3: Flowchart of the data selection process. In total 87 datasets were suitable for analysis.

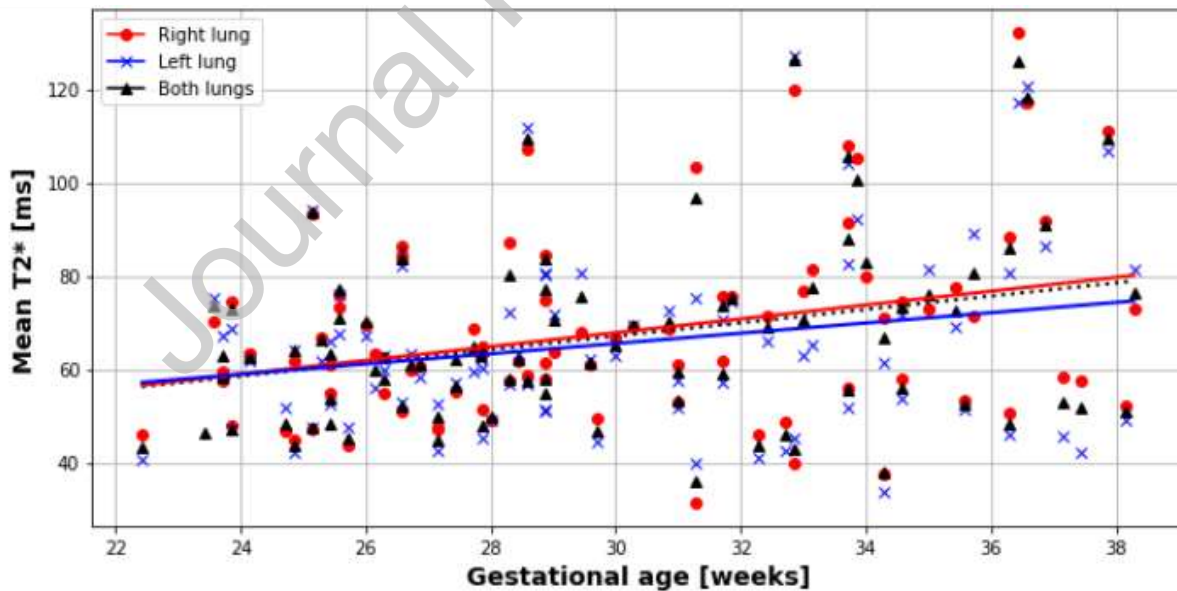


Figure 4: Mean pulmonary T2* values over gestational age at scan in right lung (red dots), left lung (blue crosses) and both lungs combined (black triangles).

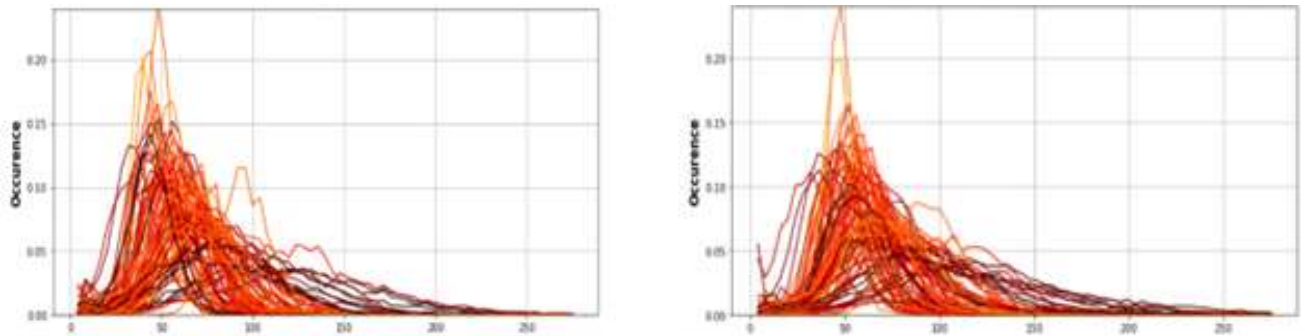


Figure 5: Histograms to illustrate the distribution of pulmonary $T2^*$ voxel values from the right (right) and left (left) lungs, from all participants, (lighter curves represent earlier gestational ages at scan).

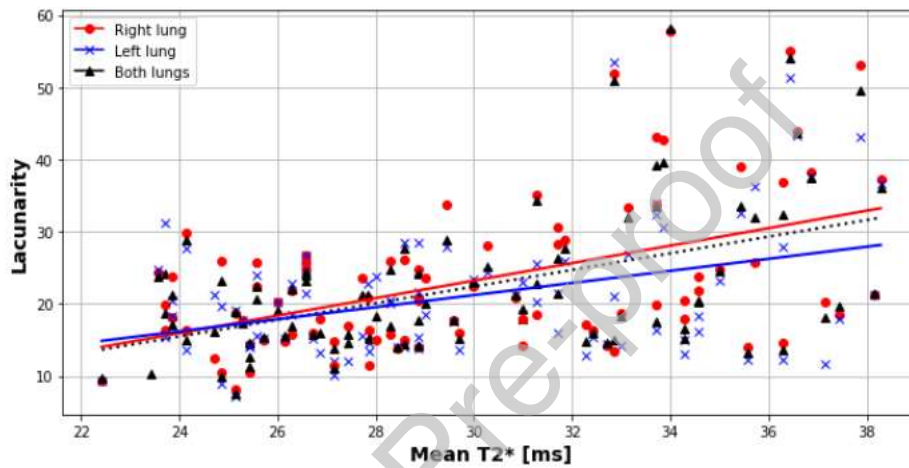


Figure 6: Scatterplot of lacunarity measure (derived from $T2^*$ mapping) for right (red dot), left (blue cross) and both lungs (black triangle).



Figure 7: T2* maps in axial, sagittal and coronal views of fetal lungs in normal pregnancies with a gestational age at scan range of 22.4-38.3. The scale of T2* values is displayed where red colours are low and yellow are high.

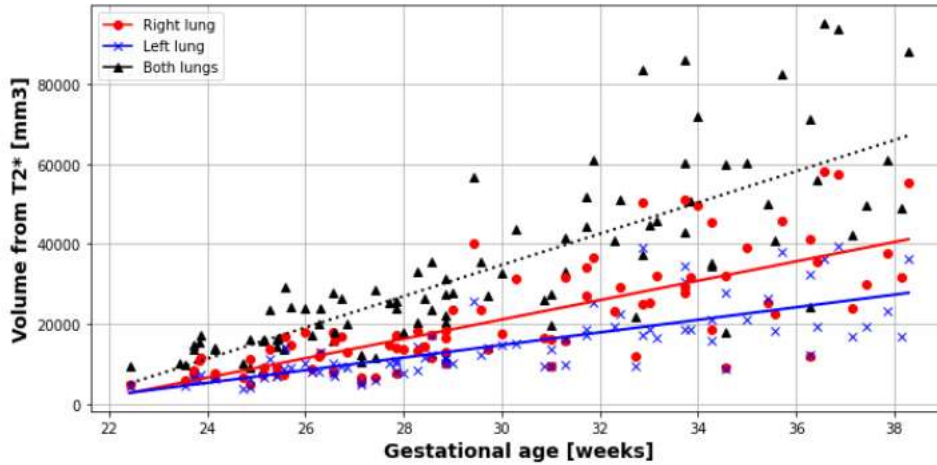


Figure 8: Pulmonary volumes over gestational age at scan in right (red dot), left (blue cross) and both lungs (black triangle).

Maternal age (years)	
Mean (SD)	34 (3.7)
Range	25-45
Ethnicity n (%)	
White	79 (91%)
Mixed	1 (1%)
Asian	5 (6%)
Black	2 (2%)
BMI (kg/m ²)	
Mean SD	22.4 (2.6)
Range	18.4-32.5
Gestational age at scan (weeks)	
Mean SD	29.9 (4.3)
Range	20.6-38.3
GA at delivery (weeks)	
Mean SD	40 (1.2)
Range	37.1-42.4

Birthweight (grams)	
Mean SD	3384 (401)
Range	2485-4400
Birthweight centile n (%)	
0-3	0 (0%)
3-10	4 (5%)
10-25	14 (16%)
25-50	20 (23%)
50-75	27 (31%)
75-90	16 (18%)
90-97	6 (7%)
97-100	0 (0%)

Table 1: Clinical characteristics study cohort